Nonlocal description of evaporating drops

J. Eggers[1] and L. M. Pismen[2]
[1]*School of Mathematics, University of Bristol, University Walk, Bristol BS8 1TW, United Kingdom*
[2]*Department of Chemical Engineering and Minerva Center for Nonlinear Physics of Complex Systems, Technion-Israel Institute of Technology, Haifa 32000, Israel*

(Received 12 May 2010; accepted 26 August 2010; published online 1 November 2010)

We present a theoretical study of the evolution of a drop of pure liquid on a solid substrate, which it wets completely. In a situation where evaporation is significant, the drop does not spread, but instead the drop radius goes to zero in finite time. Our description couples the viscous flow problem to a self-consistent thermodynamic description of evaporation from the drop and its precursor film. The evaporation rate is limited by the diffusion of vapor into the surrounding atmosphere. For flat drops, we compute the evaporation rate as a nonlocal integral operator of the drop shape. Together with a lubrication description of the flow, this permits an efficient numerical description of the final stages of the evaporation problem. We find that the drop radius goes to zero like $R \propto (t_0 - t)^{\alpha}$, where α has value close to 1/2, in agreement with experiment. © *2010 American Institute of Physics*. [doi:10.1063/1.3491133]

I. INTRODUCTION

The evaporation of liquid drops has attracted a great deal of attention recently;[1–9] see Ref. 10 for a brief review. In the case of partially wetting liquids, the contact line often remains anchored on the substrate.[1] If particles are present in the liquid, a characteristic "coffee ring" deposit is left behind as the drop dries out. Sometimes the contact line also performs a "stick-slip" motion,[3,11] leading to more complicated patterns. In the present paper, we consider the opposite case of a perfectly wetting liquid on a perfectly flat surface (e.g., droplets of water or hexane on mica), for which the effects of anchoring are negligible.

In the nonevaporating case, this implies that the drop spreads in accordance with Tanner's law. This spreading is associated with the macroscopic or apparent contact angle of the drop going to zero as the radius increases.[10] However, in the presence of significant evaporation it is observed that the macroscopic contact angle remains finite,[4] so the drop height is proportional to the drop radius. Since the drop is losing volume owing to evaporation, this can only mean that the radius is decreasing in time, and eventually goes to zero at a time t_0. In many experiments it has been observed that the vanishing of the drop radius is characterized by a power law[3–7]

$$R = \bar{R}(t_0 - t)^{\alpha}. \tag{1}$$

The experimental values for different simple liquids are found to be close to an exponent of 1/2. However, the value reported for water is 0.6.[3,7] Recent experiments[7] suggest that the difference is due to the fact that the water vapor above the droplet is being convected away because water vapor is lighter than air, contrary to the vapor of all other liquids used in the experiments. If convection of water vapor is inhibited, the exponent is once more 1/2. Thus in most cases[2,5,12] evaporation is controlled by the diffusion of vapor, and this paper will be devoted exclusively to this diffusive case. In the experimentally relevant limit[2] this means one has to solve Laplace's equation in the exterior of the drop, making the mathematical problem nonlocal.

In the present paper, as in the work cited above, the assumption will always be that the drop and the substrate are in a *local* thermodynamic equilibrium. Thus the temperature of the substrate as well as the drop assume a constant value, controlled externally, and fluid properties, such as viscosity, density, and surface tension are constant in space and time. The vapor concentration on the surface of the drop is assumed to be at the saturation concentration corresponding to the given temperature. As a result, the rate-limiting factor is the transport of vapor away from the surface. In the limit we consider here, this transport is purely diffusive. Another substantial body of work considers the situation that the temperature of the drop and/or the substrate is not constant, and nonequilibrium processes at the interface control the rate of evaporation.[9,12–18] In this situation, thermocapillary effects may be important,[16,17,19] as are the relative conductivities of substrate and liquid.[12,17]

In Ref. 2, the diffusive problem was analyzed assuming a sudden jump between the region covered by the drop, and the region exterior to the drop. Over the drop, the saturation concentration of vapor is constant to a good approximation, while in the exterior region it is assumed that the *flux* of vapor vanishes. This mixed boundary value problem[20,21] leads to a rate of evaporation which *diverges* like a square root at the edge of the drop, which is of course unphysical. In reality, the contact line region has finite width, over which the boundary condition turns gradually from one type to the other, and which regularizes the evaporative singularity. To predict the form of the regularization, one must solve the fully nonlocal problem, which couples the local contact line dynamics to the global concentration field.

To our knowledge, a self-consistent description of the nonlocal evaporation problem has never been formulated. The main objective of this paper is to provide such a descrip-

tion, and to implement it mathematically. In the next section below, we will formulate a self-consistent thermodynamic description of the evaporative problem, which includes both the drop and its exterior, covered by a thin film. In the thin drop limit we are able to express the evaporation rate as an integral over the free surface of drop and film. Details of the mathematical solution are found in the Appendix. The evaporation problem is coupled to the hydrodynamics of the drop motion, described in the lubrication approximation. In the following brief section, we describe the solution to the diffusive problem in the limit that the contact line region has zero thickness, as described previously in Ref. 2. In Sec. IV, we describe our numerical method. We show that there is a universal regime close to the point where the drop radius goes to zero, characterized by a scaling exponent α close to 1/2. However, if the drop is flat initially, it dries out into a ring before it vanishes entirely. In the final discussion we describe the structure of the asymptotic solution qualitatively and provide evidence for the self-similar nature of the contact line region.

II. THE MODEL EQUATIONS

We begin by deriving the model equations which describe evaporation from the drop and its surroundings. As discussed in Sec. I, we consider the case that evaporation is limited by diffusion. We always assume that the process is so slow that thermal gradients do not play a role and that the temperature T is constant throughout.

A. Evaporative flux

If fluid is confined to a closed container and equilibrium conditions are established, there will be no net evaporation. In the case of a macroscopic, flat interface, the mass concentration c of vapor per unit volume of air will be the saturation concentration c_{sat}. An evaporative flux arises by maintaining a nonequilibrium state: the concentration far from the drop is kept at a lower value $c_\infty < c_{\mathrm{sat}}$. The transport of liquid from the drop to infinity takes place by diffusion, where the mass flux is proportional to concentration gradients

$$\mathbf{j}_m = -D\nabla c \tag{2}$$

and where D is the diffusion constant. The distribution of concentration is governed by Laplace's equation

$$\Delta c = 0 \tag{3}$$

assuming a slow process of evaporation.

To compute the mass flux $\mathbf{n}\cdot\mathbf{j}_m$ from the fluid surface (and where $\mathbf{n}$ is the outward normal), one has to solve Eq. (3) for the distribution of c with suitable boundary conditions. Apart form the condition $c=c_\infty$ at infinity, boundary conditions are that the immediate neighborhood of the fluid surface is at a concentration c_v. For a flat, macroscopic fluid film this concentration would be $c_v=c_{\mathrm{sat}}$. If however the interface is curved, Kelvin's equation[5,22] shows that the concentration is in fact modified

$$\ln\frac{c_v}{c_{\mathrm{sat}}} = \frac{M}{\rho R_u T}[\gamma\kappa - \Pi(h)], \tag{4}$$

where γ is the surface tension and κ the curvature of the interface. The expression in brackets represents the change of the chemical potential at the interface due to curvature and to interaction with the substrate.[23] In the classical case of a spherical drop we have $\kappa>0$, so the vapor pressure is increased. As a result, a small enough drop will shrink, when the vapor pressure around the drop is greater than the ambient vapor pressure.

The prefactor is computed from the molar mass M, universal gas constant R_u, and fluid density ρ. If the film is very thin, one must also take the disjoining pressure Π into account. For the perfectly wetting liquids to be considered here, van der Waals forces are repulsive, and we have[10]

$$\Pi = \frac{A}{6\pi h^3} \equiv \gamma\frac{a^2}{h^3}. \tag{5}$$

Here $A>0$ is the Hamaker constant and a comes out to be a microscopic length.[10] Under typical experimental conditions, we can consider the linearized version of Eq. (4)

$$c_v = c_{\mathrm{sat}} + \frac{Mc_{\mathrm{sat}}}{\rho R_u T}[\gamma\kappa - \Pi(h)]. \tag{6}$$

Far from the drop, there is only a thin adsorbed film of liquid.[6] Its thickness h_f is determined by the condition that $c_v=c_\infty$, so that there is no evaporation. This means we can write

$$\bar{c} \equiv c_v - c_\infty = \frac{Mc_{\mathrm{sat}}\gamma}{\rho R_u T}\left(\kappa - \frac{a^2}{h^3} + \frac{a^2}{h_f^3}\right), \tag{7}$$

where $\bar{c}$ was chosen to *vanish* at infinity. These boundary conditions determine a solution $c(r,z)$ of Eq. (3) completely, where z is the distance from the solid plate and r is the radial distance from the center of the drop. The flux from the fluid surface is then determined by Eq. (2).

To simplify the problem, we will consider the case that the drop is thin. This permits us to use lubrication theory,[24] and to solve the diffusion problem directly in terms of $\bar{c}$, defined on the drop surface. Namely, in the limit of a thin drop we only have to solve Eq. (3) in half-space, with $\bar{c}(r)$ specified on the plane $z=0$. Using the same approximation, the *volume* flux from the surface becomes

$$j_{ev} = -\frac{D}{\rho}\frac{\partial c}{\partial z}. \tag{8}$$

Details of the calculation are relegated to the Appendix, but the result is that j_{ev} can also be expressed as an integral over $\bar{c}(r)$ specified on the plane $z=0$. We find that j_{ev} is best computed via the *total* evaporation up to some radius r

$$J_{ev} = \int_0^r r j_{ev} dr = -\frac{D}{\rho}\int_0^\infty K(r,r')\frac{\partial\bar{c}}{\partial r'}dr' \tag{9}$$

so that

$$j_{ev} = \frac{1}{r}\frac{\partial J_{ev}}{\partial r}. \tag{10}$$

The kernel is given by

$$K(r,r') = \frac{2}{\pi}\begin{cases} r[\mathbf{K}(r'/r) - \mathbf{E}(r'/r)], & r' < r \\ r'[\mathbf{K}(r/r') - \mathbf{E}(r/r')], & r' > r \end{cases}, \tag{11}$$

where **K** and **E** are the complete elliptic integrals, defined as[25]

$$\mathbf{K}(x) = \int_0^{\pi/2} \frac{d\theta}{\sqrt{1 - x^2 \sin^2\theta}},$$
$$\mathbf{E}(x) = \int_0^{\pi/2} \sqrt{1 - x^2 \sin^2\theta}\, d\theta. \tag{12}$$

B. Viscous transport

Now we are in a position to solve for the fluid flow inside the drop and thus to deduce the free-surface motion of its surface. Evaporation is taken into account through the mass flux (10) alone. Inside the drop, we solve the viscous flow equations appropriate for slow (Stokes) flow.[26] The boundary conditions on the solid surface are those of no slip, and of continuity of stress on the free surface. The description can be simplified greatly in the so-called lubrication approximation, valid for small and slowly varying slope of the interface.[10] This is a good approximation for most evaporation experiments. The idea is to regard the solid and the free surface as nearly parallel, in which case the flow profile becomes parabolic[27]

$$u_r = \frac{1}{2\eta}\frac{\partial p}{\partial r}[y^2 - 2h(r)y]. \tag{13}$$

Here y is the distance from the solid plate and η the viscosity. In deriving Eq. (13), we have used the no slip condition on the solid surface and the condition of vanishing shear stress on the free surface.

The dynamic pressure, whose gradients drive the flow, is given by

$$p = \gamma\kappa - \frac{A}{6\pi h^3} = -\gamma\left(\frac{\partial^2 h}{\partial r^2} + \frac{1}{r}\frac{\partial h}{\partial r} + \frac{a^2}{h^3}\right). \tag{14}$$

For simplicity, we have neglected gravity, which is a good approximation for small drops, smaller than the capillary length $\ell_c = \sqrt{\gamma/\rho g}$. It is a simple matter to include gravity if needed. The great advantage of the lubrication approach is that Eq. (13) is an explicit expression for the (radial) velocity field. The condition of mass balance (continuity equation) now yields an equation of motion for the thickness $h(r,t)$ of the drop[10]

$$\frac{\partial h}{\partial t} + \frac{1}{r}\frac{\partial (jr)}{\partial r} = -j_{ev}(r). \tag{15}$$

The second term on the left is due to viscous transport

$$j = \frac{v_\eta h^3}{3}\frac{\partial}{\partial r}\left(\frac{\partial^2 h}{\partial r^2} + \frac{1}{r}\frac{\partial h}{\partial r} + \frac{a^2}{h^3}\right) \tag{16}$$

in the liquid film, and where $v_\eta = \gamma/\eta$ is the capillary speed. For water, $v_\eta = 7.3 \times 10^4$ cm/s. The right of Eq. (15) represents the *volume* flux per unit area due to evaporation. The viscous transport is driven by gradients of the pressure in the film. Since our description includes regions where the liquid film is very thin, we have included disjoining pressure. Thus to summarize, we have to solve the coupled set of Eqs. (7), (9), (10), (15), and (16) for the variables $\bar{c}$, j_{ev}, h, and j.

III. THE EVAPORATIVE SINGULARITY

It was realized by Ref. 2 that the form of j_{ev}, except for a small region around the contact line, can be found from the following simple observations. First, one finds that over the drop surface, $\bar{c}$ is dominated by the last term a^2/h_f^3 in Eq. (7), which is the inverse of a microscopic length. Except very close to the contact line, a^2/h^3 vanishes very quickly as h becomes macroscopic. Thus in the interior of the drop $\bar{c} = c_s$, where

$$c_s = \frac{M c_{\mathrm{sat}} \gamma a^2}{\rho R_u T h_f^3}. \tag{17}$$

It is much more difficult to guess the form of $\bar{c}$ in the exterior of the drop. Instead,[2] noticed that a more suitable boundary condition for the large-scale profile is that the evaporation rate j_{ev} has to vanish in the exterior of the drop.

Thus the outer problem for the evaporation is to be formulated as a *mixed* boundary value problem for the fields $\bar{c}$ and j_{ev}, which are connected by the condition (8). For $r < R$, the boundary condition is $\bar{c} = c_s$, for $r > R$, the boundary condition is $j_{ev} = 0$. In the half space $z > 0$, Laplace's equation $\Delta c = 0$ is to be solved. According to Ref. 20, the result is

$$j_{ev} = \begin{cases} \dfrac{2\beta}{\pi\sqrt{R^2 - r^2}} & r < R \\ 0 & r \geq R \end{cases},$$
$$\bar{c} = c_s \begin{cases} 1 & r < R \\ \dfrac{2}{\pi}\arcsin\left(\dfrac{R}{r}\right) & r \geq R \end{cases}, \tag{18}$$

where

$$\beta = \frac{D c_s}{\rho}. \tag{19}$$

Integrating the flux over the drop one finds

$$J_{tot} = 2\pi\int_0^R j_{ev} r dr = 4\beta R \tag{20}$$

which shows that the total volume flux of vapor from the drop is proportional to the radius of the drop, not its surface area.[2] Under typical conditions for the evaporation of a water drop at room temperature, $\beta = 4 \times 10^{-6}$ cm^2/s.[2] We mention that it is a misconception to believe that the proportionality

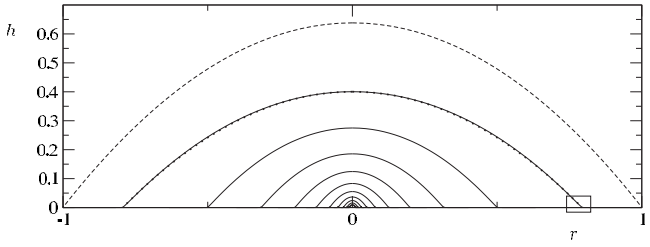

FIG. 1. A typical simulation, with parameters (all in units of R_0 and R_0/v_η) $a=10^{-3}$, $h_f=5\times10^{-5}$, and $\beta=0.005$. The initial condition is shown as the dashed line. For one of the profiles, dots show the static drop shape [Eq. (36)] for comparison. The contact line region of this profile, shown on an expanded scale in Fig. 2, is marked by a box. Outside of the drop, the substrate is covered by a thin precursor film.

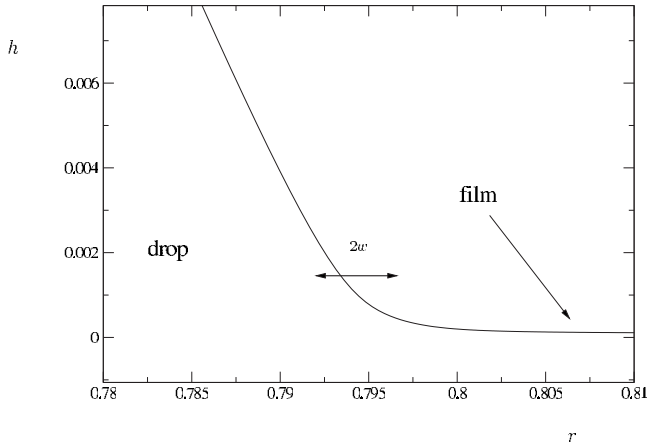

FIG. 2. Closeup of the contact line region marked by a box in Fig. 1, which describes the crossover between the precursor film and the drop. The size $2w$ of this region, defined by the half-width w of the peak of the capillary pressure, is marked by the arrow. The behavior of w as function of the drop radius is shown in Fig. 7 below.

of the flux to the radius is a result of the divergence of j_{ev} near the contact line. Namely, the evaporation from a spherical drop (suspended in air) is also proportional to R. This follows from the solution of Laplace's equation $\bar{c}=c_sR/r$, where r is the distance from the drop's center, and which obeys the boundary condition $\bar{c}=c_s$ on the drop surface. But this means that the normal flux is

$$\mathbf{n}\cdot\mathbf{j}_{ev}=-\frac{D}{\rho}\frac{\partial\bar{c}}{\partial r}=\frac{\beta}{R} \tag{21}$$

and $J_{\mathrm{tot}}=4\pi\beta R$. Thus in absence of a contact line the form of Eq. (20) remains the same, although the prefactor is modified.

Once the outer solution (18) is known, one can deduce the asymptotics of the profile $h(r)$ far from the drop. According to Eq. (18), $\bar{c}(r)$ decays like $\bar{c}(r)\approx 2c_sR/(\pi r)$ for $r\gg R$. Also, the effects of curvature will be small in the exterior part of the drop, so we may write

$$\bar{c}=c_s\left(1-\frac{h_f^3}{h^3}\right). \tag{22}$$

Hence the asymptotic behavior of h becomes

$$h(r)\approx h_f\left(1+\frac{2R}{3\pi r}\right),\quad r\gg R. \tag{23}$$

This is the boundary condition we will impose on the liquid film surrounding the drop. As expected, the thickness converges to the constant value h_f sufficiently far from the drop.

IV. SIMULATION

We are now in a position to treat the coupled set of Eqs. (15), (16), (9)–(11), and (22) numerically. For simplicity, we use the form (22) for the concentration $\bar{c}$ instead of Eq. (7), since van der Waals forces dominate in the contact line region. At this point it is worthwhile to recall the equations being solved in a more compact from. They are

$$\frac{\partial h}{\partial t}+\frac{v_\eta}{r}\frac{\partial}{\partial r}\left[\frac{h^3r}{3}\frac{\partial}{\partial r}\left(\frac{\partial^2h}{\partial r^2}+\frac{1}{r}\frac{\partial h}{\partial r}+\frac{a^2}{h^3}\right)\right]=-j_{ev}, \tag{24}$$

$$j_{ev}=\frac{\beta}{r}\frac{\partial}{\partial r}\left[\int_0^\infty K(r,r')\frac{\partial}{\partial r'}\left(\frac{h_f}{h}\right)^3dr'\right]. \tag{25}$$

As units of length we use the initial drop radius R_0, as the unit of time we choose R_0/v_η. We use a fully implicit finite difference method, similar to that employed in Ref. 28. The grid is staggered, node points for h being defined on the grid, node points for the flux j being defined in the middle between two grid points. The integral (9) is evaluated in between grid points using the midpoint rule. To treat the singularity in the kernel (11) that occurs for $r'\approx r$, for each r we cut out a region of integration $[r-\delta_1,r+\delta_2]$ of about 20 grid spacings. Inside this region, we approximate Eq. (11) by

$$K(r,r')\approx\frac{r}{\pi}\ln|r'-r| \tag{26}$$

and treat $\bar{c}$ as a constant. The integral over $[r-\delta_1,r+\delta_2]$ is then evaluated analytically.

We choose the simulation domain to be about 100 times larger than the initial drop radius. For the boundary condition at the last grid point $x(k)$ (where k is the total number of points), we use the asymptotic representation (23). To evaluate J_{ev} beyond $x(k)$, we use Eq. (23) as well as the asymptotic representation

$$K(r,r')\approx\frac{r^2}{2r'} \tag{27}$$

valid for $r'\gg r$. Finally, to compute the rate of evaporation j_{ev} at the origin $r=0$, we use

$$j_{ev}(0)=-\int_0^\infty\frac{1}{r'}\frac{\partial\bar{c}}{\partial r'}dr' \tag{28}$$

which follows from Eqs. (27) and (10). We choose a strongly graded grid, which has most of its resolution concentrated at the edge of drop, where the grid size is a fraction of the film thickness h_f, and is kept constant over the contact line region. Outside of the contact line region, the grid spacing is allowed to vary by 5% from one grid point to the next. In particular, in the thin film region far from the drop the grid spacing becomes up to $5R_0$.

In Fig. 1 we show a sequence of drop profiles resulting

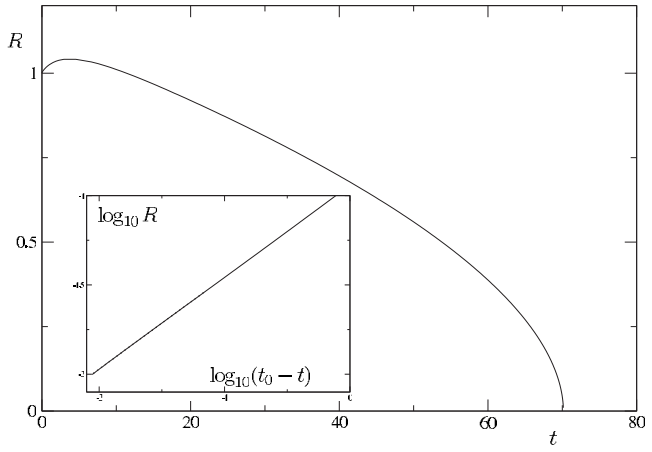

FIG. 3. The drop radius R as function of time, using the same simulation as shown in Fig. 1; in the inset, we also plot $\log_{10} R$ as function of $\log_{10}(t_0-t)$, together with a best fit (dotted line). The asymptotic behavior is $R=0.114t'^{0.515}$.

from a typical simulation. The initial condition is shown as the dotted line. Without evaporation, the surface potential corresponds to a situation of complete wetting, and the drop should spread.[10] However, consistent with experiment, the drop evaporates while appearing to meet the substrate at a finite angle. This angle is the so-called apparent contact angle θ_{ap}, discussed in more detail in Sec. V. However, an expanded view of the contact line region, shown in Fig. 2, reveals that the slope in fact changes continuously, and that substrate in the exterior of the drop is covered by a thin film. As a result of the apparent contact angle being finite, the radius of the drop goes to zero in finite time, as seen in Fig. 3. After an initial small increase, the drop radius vanishes at $t_0=70.142$. In the inset, we use a double logarithmic plot to demonstrate that the radius goes to zero with the power law (1). A best fit to the data shows that the power is close to $\alpha=1/2$, as expected from experimental data.[7] For our choice of parameters, the slope of the profile is safely below unity, so it is consistent to use a lubrication approximation, as we do.

It is also instructive to consider the evaporation rate j_{ev} as computed self-consistently by our numerical procedure. We use the same simulation as shown in Fig. 1, and plot profiles of j_{ev} and $\bar{c}$ for $R=0.505$. On the left of Fig. 4, we show the evaporation rate, which has a square-root singularity according to the macroscopic theory represented by Eq. (18). Indeed, the numerical solution follows the expression (18) rather closely, but ultimately the singularity is rounded. This is due to the fact that the contact line region is in fact of finite size, as we will see in more detail below. In the exterior of the drop, one observes the slow decay of the concentration field $\bar{c}$, again in good agreement with theory.

As is typical for a power law, we expect the final stage of drop evaporation to be independent of initial conditions. This hypothesis is tested in Fig. 5. While keeping all parameters constant, the initial condition was changed, considering drops of widely different volumes. For example, for large initial drop volume, the drop first spreads before it starts to shrink. However, as the drop radius goes to zero, the relationship between the drop thickness and its radius becomes identical (solid lines). It can of course be checked that the entire drop shape is universal, independent of initial conditions. However, if the drop is made too thin, it will dry out first in the middle, as shown in Fig. 6. This behavior, which belongs to a different class of asymptotic behaviors, is shown as the dashed line in Fig. 5. First, the profile develops a minimum in the center of the drop. Before the edge of the drop can recede, it dries out completely (save of course for a thin film), forming a toroidal shape. Eventually, the entire drop disappears. To avoid confusion, we stress that the toroidal shape discussed here is not related to ring-shaped deposits formed in the case of contact line anchoring.[3]

At the bottom of Fig. 6, we show the corresponding local evaporation rate. As long as the drop thickness is still macroscopic, the evaporation rate is hardly affected by the dimple that has formed in the middle of the drop. Thus as predicted by Eq. (18), j_{ev} continues to *increase* in the center as R decreases. On the other hand since the drop is thin, viscous transport [Eq. (16)] is small, and fluid at the center of the drop is not replenished, leading to drying. Only when there is nothing but a thin film left in the middle of the drop does j_{ev} go to zero in the center. This shows that there is a more complicated set of attractors for the evaporation dy-

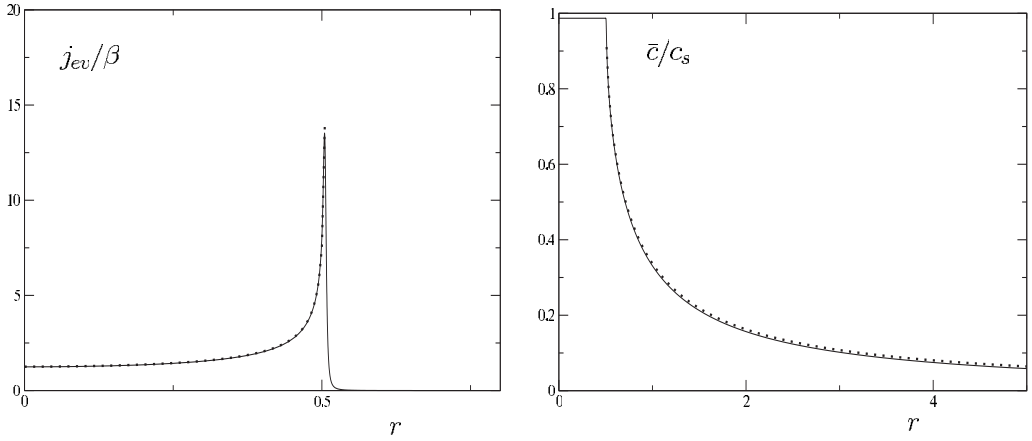

FIG. 4. The evaporation rate j_{ev}/β on the left, and the concentration $\bar{c}/c_s$ on the right. The dotted lines are the asymptotic results [Eq. (18)].

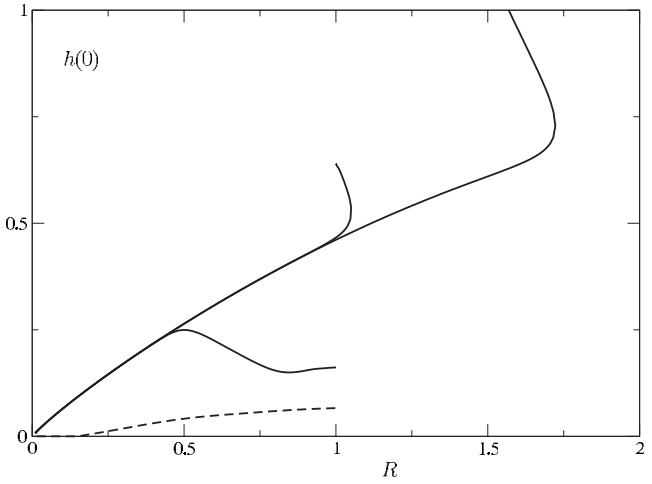

FIG. 5. A plot of the drop height $h(0)$ as function of the radius, in units of the initial drop radius R_0. The parameters are $a=10^{-3}$, $h_f=10^{-4}$, and $\beta=0.005$. By definition, $R_0=1$ for each run, but the initial drop height $h(0)$ is decreasing, as drop volumes are chosen as $V=4$, $V=1$, $V=1/4$, and $V=1/10$. For the first three runs, the asymptotic behavior for small R is always the same. However, the thinnest drop dries in the middle (dashed line), as shown in Fig. 6 below.

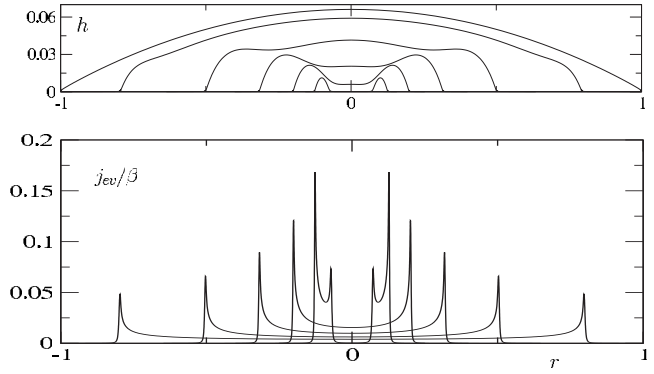

FIG. 6. A simulation with the same parameters as in Fig. 5, but with a much thinner drop as initial condition ($V=1/10$). The drop dries in the middle to from a ring (top panel). The bottom panel shows the rate of evaporation.

namics than anticipated. Presumably, each is characterized by a universal dynamics close to the disappearance of the drop, as demonstrated for the simplest case without dry spots in Fig. 5 above. However, it is worth remarking that the evaporation rate of $\beta=0.005$ used in Fig. 6 is far larger than that realized in a typical experiment. Thus, although interesting theoretically, drying may not be observable experimentally.

Following this discussion of the qualitative behavior of the dynamics we analyze the full range of possible parameters that determine drop behavior. The problem is controlled by the relative evaporation rate β, the capillary speed v_η, the van der Waals length a, and the film thickness h_f. Evidently, this leads to a set of two dimensionless parameters, which fully determine the problem

$$d_1 = \frac{\beta}{a v_\eta}, \quad d_2 = \frac{a}{h_f}. \tag{29}$$

More information is obtained by recasting the solution in dimensionless form

$$h(r,t) = h_f \tilde{h}(r/\ell, t/\tau) \equiv h_f \tilde{h}(\tilde{r},\tilde{t}). \tag{30}$$

With the choice of radial length scale $\ell = v_\eta a^2/\beta$ and time scale $\tau = v_\eta a^2 h_f/\beta^2$, the equations of motion become

$$\frac{\partial \tilde{h}}{\partial \tilde{t}} + \frac{1}{3\tilde{r}}\frac{\partial}{\partial \tilde{r}}\left[\tilde{h}^3 \frac{\partial}{\partial \tilde{r}}\left(\Xi^2 \Delta \tilde{h} + \frac{1}{\tilde{h}^3}\right)\tilde{r}\right] = -\tilde{j}_{ev}(\tilde{r}) \tag{31}$$

with

$$\tilde{j}_{ev}(\tilde{r}) = -\frac{1}{\tilde{r}}\frac{\partial}{\partial \tilde{r}}\left[\int_0^\infty K(\tilde{r},r')\frac{\partial \tilde{c}}{\partial r'}dr',\right] \tag{32}$$

and

$$\tilde{c} = 1 - 1/\tilde{h}^3. \tag{33}$$

Thus after the rescaling Eq. (30), there remains only a single parameter

$$\Xi = \frac{h_f^2 \beta}{a^3 v_\eta} = \frac{d_1}{d_2^2} \tag{34}$$

in the equations of motion. The dependence on the second dimensionless parameter only appears in the initial conditions. This is of significance for the asymptotic regime close to the disappearance of the drop, which is *independent* of initial conditions. We have thus shown that the final regime only depends on the parameter Ξ, up to rescaling.

V. DISCUSSION

We now outline the overall structure of the evaporation problem as relevant to experiment. It is important to note that most experiments take place in a regime where viscous transport dominates over evaporation, as seen by considering the balance Eq. (15). Over the scale of the drop j_{ev} is given by Eq. (18). Thus the evaporation scales like β/R, while the order of magnitude of viscous transport is v_η. Here we have assumed that all lengths are of order R. This means that there is critical drop radius

$$R_{cr} = \beta/v_\eta \tag{35}$$

below which evaporation dominates the dynamics of the drop. However, for typical evaporation experiments with water $R_{cr} \approx 2.3 \times 10^{-4}$ cm, so the relevant scaling regime is one where viscous transport is dominant inside the drop, and on which we are focusing here.

Nevertheless, it is worth mentioning that formally there is a final asymptotic regime where the drop dynamics is dominated completely by evaporation, and we explain briefly the scaling for this case. In the asymptotic limit the drop is no longer flat, but rather the macroscopic drop shape is a half sphere, in which case the evaporation problem can be solved exactly, since it is the same as the evaporation of a full sphere. This is because the flux in the plane of the equator vanishes by symmetry. Thus we obtain our earlier result [Eq. (21)] for the normal flux, and we note that a half sphere is indeed a self-consistent solution. Now mass balance requires

that $\dot{R}=-\beta/R$, with solution $R=\sqrt{2\beta(t-t_0)}$. In other words, the scaling exponent α is exactly 1/2 in this case.

Now we return to the case of "slow" evaporation $R>R_{cr}$, which is also realized in our numerical simulations. Strong viscous transport means that the shape of the drop approaches that of a capillary equilibrium surface

$$h(r)=\frac{2V}{\pi R^2}\left[1-\left(\frac{r}{R}\right)^2\right]. \tag{36}$$

As shown in Fig. 1 for the profile with $R\approx 0.8$, this is an excellent approximation, since $R_{cr}=0.005\ll R$. The volume V is of course not a constant, but decreases with evaporation. Using the total evaporation (20) it follows that

$$\dot{V}=-4\beta R. \tag{37}$$

The angle at which the macroscopic shape [Eq. (36)] intersects with the solid is called the apparent contact angle θ_{ap},[10] and

$$V=\frac{\pi}{4}R^3\theta_{ap}. \tag{38}$$

It is a simple matter to check that *if* the apparent contact angle is constant, the scaling exponent must be $\alpha=1/2$. However, the real challenge is of course to show that θ_{ap} indeed remains finite as the drop shrinks to zero. To this end it seems inevitable to understand the local structure of the solution close to the contact line. In the present case, this task is complicated by the fact that the problem is nonlocal. As usual, we make the traveling wave ansatz

$$h(r,t)=h_f H\left[\frac{r-R(t)}{w}\right]\equiv H(\zeta), \tag{39}$$

where w is the width of contact line region. A similar structure is expected to hold for j_{ev}. For large negative values of $\zeta=[r-R(t)]/w$ the similarity form must match to Eq. (18). If one expands Eq. (18) for small w, one finds

$$j_{ev}\approx\frac{\sqrt{2\beta}}{\pi\sqrt{-wR\zeta}},\quad \zeta\to-\infty.$$

This means the similarity form of j_{ev} is

$$j_{ev}=\frac{\beta}{\sqrt{wR}}J(\zeta). \tag{40}$$

In the lubrication Eq. (15), j_{ev} is expected to balance with van der Waals forces, which are large in the contact line region. Using the similarity form (39) and $r\approx R$, the contribution to $\partial j/\partial r$ coming from van der Waals forces is estimated to be

$$\frac{v_\eta a^2}{3}\frac{\partial}{\partial r}\left(h^3\frac{\partial h^{-3}}{\partial r}\right)=-\frac{v_\eta a^2}{w^2}(H_\zeta/H)_\zeta. \tag{41}$$

Balancing this with Eq. (40) we arrive at the estimate

$$w\approx\left(\frac{v_\eta a^2}{\beta}\right)^{2/3}R^{1/3} \tag{42}$$

for the width of the contact line region. For the parameters of Fig. 1 this leads to $w\approx 0.0034R^{1/3}$, which agrees nicely with the best fit determined from numerical data, cf. Figure 7.

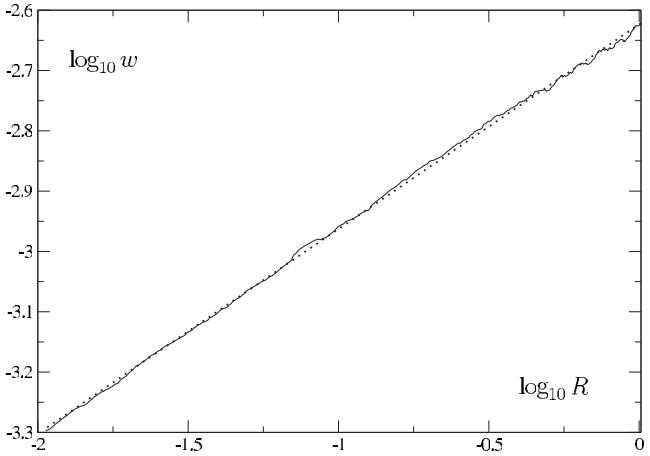

FIG. 7. The width w of the contact line region as function of the drop radius R in a double logarithmic plot. Numerically, w is defined as the half-width of the peak the capillary pressure has at the contact line. The simulation is the same as shown in Fig. 1. The dotted line is a best fit corresponding to $w=0.002\,38R^{0.339}$.

These results clearly demonstrates the existence of a local similarity structure. The next step is to formulate a local equation in similarity variables, valid near the contact line. We expect a solution of this problem to yield an expression for θ_{ap}, which would in principle close the problem. However, we have so far been unable to formulate such a local problem, and both the local solution and the behavior in the far field appears to be coupled.

ACKNOWLEDGMENTS

This research was supported in part by the Project of Knowledge Innovation Program (PKIP) of the Chinese Academy of Sciences. The authors are thankful for the hospitality of the Kavli Institute for Theoretical Physics China, CAS, Beijing, Institut Poincaré, Paris, and IMA, Minneapolis, which has made this cooperation possible. We also acknowledge illuminating discussions with Daniel Bonn and Marco Fontelos. L.M.P. acknowledges support by the European Union under Grant No. PITN-GA-214919.

APPENDIX: EVAPORATION INTEGRAL

We would like to solve Laplace's equation in half-space, for a concentration field c which vanishes at infinity. A radially symmetric distribution $c(r)$ is prescribed in the plane $z=0$. We seek a solution of Laplace's Eq. (3) by writing the concentration in all of space in the form[20]

$$c(r,z)=\int_0^\infty e^{-kz}J_0(kr)a(k)dk, \tag{A1}$$

where $a(k)$ is an amplitude to be determined. From Eqs. (A1) and (8) it follows that the evaporation rate on the surface is

$$j_{ev}(r)=\frac{D}{\rho}\int_0^\infty kJ_0(kr)a(k)dk. \tag{A2}$$

Now

$$\int_0^\infty rc(r,0)J_0(qr)dr = \int_0^\infty \int_0^\infty J_0(kr)a(k)rJ_0(qr)drdk$$

$$= \int_0^\infty \frac{a(k)}{k}\delta(k-q)dk \tag{A3}$$

using the well-known orthogonality relation for Bessel functions. Thus the amplitude can be written as

$$a(q) = q\int_0^\infty r'c(r')J_0(qr')dr' \tag{A4}$$

and inserting this into Eq. (A2) yields

$$j_{ev}(r) = \frac{D}{\rho}\int_0^\infty \int_0^\infty r'c(r')J_0(kr')k^2J_0(kr)dkdr'. \tag{A5}$$

However, Eq. (A5) needs to be treated with care, since the asymptotic behavior of the Bessel function is[29]

$$J_n(x) \approx \sqrt{\frac{2}{\pi x}}\cos\left(x - \frac{n\pi}{2} - \frac{\pi}{4}\right), \tag{A6}$$

so the integral over k diverges strongly for large k.

It is thus necessary to rewrite Eq. (A5) to improve convergence. Namely, using

$$\frac{d}{dr'}\left[\frac{r'}{k}J_1(kr')\right] = r'J_0(kr') \tag{A7}$$

one finds integrating by parts

$$j_{ev}(r) = -\frac{D}{\rho}\int_0^\infty \int_0^\infty r'kJ_1(kr')J_0(kr)\frac{\partial c}{\partial r'}dr'dk \tag{A8}$$

and integrating a second time

$$J_{ev} = \int_0^r rj_{ev}(r)dr$$

$$= -\frac{D}{\rho}\int_0^\infty \int_0^\infty rr'J_1(kr')J_1(kr)\frac{\partial c}{\partial r'}dr'dk. \tag{A9}$$

Comparing with Eq. (9) we identify

$$K(r,r') = \int_0^\infty rr'J_1(kr')J_1(kr)dk \tag{A10}$$

which is convergent owing to the oscillatory factor in Eq. (A6), provided that $r \neq r'$.

Now the integral over k can be performed using[30] (p. 410).

$$\int_0^\infty J_1(at)J_1(bt)dt$$

$$= \frac{b\Gamma(3/2)}{a^2\Gamma(2)\Gamma(1/2)}F(3/2,1/2;2,b^2/a^2), \quad a > b, \tag{A11}$$

where F is the hypergeometric function.[29]

Putting $\alpha=3/2$, $\beta=1/2$, $\gamma=1$, and $z=a^2$ in Gauss' recursion function (see Ref. 25, p. 1045).

$$\gamma F(\alpha,\beta;\gamma,z) - \gamma F(\alpha,\beta+1;\gamma,z) + \alpha zF$$
$$\times(\alpha+1,\beta+1;\gamma+1,z) = 0 \tag{A12}$$

and expressing the complete elliptic integrals in terms of the hypergeometric function,[25] p. 905

$$\mathbf{E}(a) = \frac{\pi}{2}F\left(-\frac{1}{2},\frac{1}{2};1,a^2\right), \quad \mathbf{K}(a) = \frac{\pi}{2}F\left(\frac{1}{2},\frac{1}{2};1,a^2\right) \tag{A13}$$

we obtain

$$F(3/2,1/2;2,a^2) = \frac{4}{a^2\pi}[\mathbf{K}(a) - \mathbf{E}(a)]. \tag{A14}$$

Combining Eqs. (A10), (A11), and (A14), we find the result Eq. (11) as cited above.

[1] R. D. Deegan, O. Bakajin, T. F. Dupont, G. Huber, S. R. Nagel, and T. A. Witten, "Capillary flow as the cause of ring stains from dried liquid drops," Nature **389**, 827 (1997).
[2] R. D. Deegan, O. Bakajin, T. F. Dupont, G. Huber, S. R. Nagel, and T. A. Witten, "Contact line deposits in an evaporating drop," Phys. Rev. E **62**, 756 (2000).
[3] R. D. Deegan, "Pattern formation in drying drops," Phys. Rev. E **61**, 475 (2000).
[4] M. Cachile, O. Benichou, and A.-M. Cazabat, "Evaporating droplets of completely wetting liquids," Langmuir **18**, 7985 (2002).
[5] M. Cachile, O. Benichou, C. Poulard, and A.-M. Cazabat, "Evaporating droplets," Langmuir **18**, 8070 (2002).
[6] C. Poulard, O. Benichou, and A.-M. Cazabat, "Freely receding evaporating droplets," Langmuir **19**, 8828 (2003).
[7] N. Shahidzadeh-Bonn, S. Rafaï, A. Azouni, and D. Bonn, "Evaporating droplets," J. Fluid Mech. **549**, 307 (2006).
[8] C. Poulard, G. Guena, A.-M. Cazabat, A. Boudaoud, and M. Ben Amar, "Rescaling the dynamics of evaporating drops," Langmuir **21**, 8226 (2005).
[9] N. Murisic and L. Kondic, "Modeling evaporation of sessile drops with moving contact lines," Phys. Rev. E **78**, 065301 (2008).
[10] D. Bonn, J. Eggers, J. Indekeu, J. Meunier, and E. Rolley, "Wetting and spreading," Rev. Mod. Phys. **81**, 739 (2009).
[11] S. Maheshwari, L. Zhang, Y. Zhu, and H.-C. Chang, "Coupling between precipitation and contact-line dynamics: Multiring stains and stick-slip motion," Phys. Rev. Lett. **100**, 044503 (2008).
[12] K. Sefiane, S. K. Wilson, S. David, G. J. Dunn, and B. R. Duffy, "On the effect of the atmosphere on the evaporation of sessile droplets of water," Phys. Fluids **21**, 062101 (2009).
[13] D. M. Anderson and S. H. Davis, "The spreading of volatile liquid droplets on heated surfaces," Phys. Fluids **7**, 248 (1995).
[14] L. M. Hocking, "On contact angles in evaporating liquids," Phys. Fluids **7**, 2950 (1995).
[15] S. J. S. Morris, "A phenomenological model for the contact region of an evaporating meniscus on a superheated slab," J. Fluid Mech. **411**, 59 (2000).
[16] R. M. Ybarra and P. Neogi, "Dynamic contact angles under evaporation," J. Chem. Phys. **120**, 5755 (2004).
[17] W. D. Ristenpart, P. G. Kim, C. Domingues, J. Wan, and H. A. Stone, "Influence of substrate conductivity on circulation reversal in evaporating drops," Phys. Rev. Lett. **99**, 234502 (2007).
[18] C. Sodtke, V. S. Ajaev, and P. Stephan, "Dynamics of volatile liquid droplets on heated surfaces: Theory versus experiment," J. Fluid Mech. **610**, 343 (2008).
[19] J. P. Burelbach, S. G. Bankoff, and S. H. Davis, "Nonlinear stability of evaporating/condensing liquid films," J. Fluid Mech. **195**, 463 (1988).
[20] J. D. Jackson, *Classical Electrodynamics* (Wiley, New York, 1975).
[21] I. N. Sneddon, *Elements of Partial Differential Equations* (McGraw-Hill, New York, 1957).

[22]E. A. Guggenheim, *Thermodynamics* (North Holland, Amsterdam, 1967).
[23]L. M. Pismen, "Spinodal dewetting in a volatile liquid film," Phys. Rev. E **70**, 021601 (2004).
[24]A. Oron, S. H. Davis, and S. G. Bankoff, "Long-scale evolution of thin liquid films," Rev. Mod. Phys. **69**, 931 (1997).
[25]I. S. Gradshteyn and I. M. Ryzhik, *Table of Integrals Series and Products* (Academic, New York, 1980).
[26]L. D. Landau and E. M. Lifshitz, *Fluid Mechanics* (Pergamon, Oxford, 1984).
[27]G. K. Batchelor, *An Introduction to Fluid Dynamics* (Cambridge University Press, Cambridge, 1967).
[28]J. Eggers and T. F. Dupont, "Drop formation in a one-dimensional approximation of the Navier–Stokes equation," J. Fluid Mech. **262**, 205 (1994).
[29]M. Abramowitz and I. A. Stegun, *Handbook of Mathematical Functions* (Dover, New York, 1968).
[30]G. N. Watson, *A Treatise on the Theory of Bessel Functions* (Cambridge University Press, Cambridge, 1962).